2D-DIGE analysis of ovarian cancer cell responses to cytotoxic gold compounds

Molecular BioSystems

Dynamic Article Links

Cite this: *Mol. BioSyst.*, 2012, **8**, 985–993

www.rsc.org/molecularbiosystems

PAPER

2D-DIGE analysis of ovarian cancer cell responses to cytotoxic gold compounds†

Francesca Guidi,‡[ab] Michele Puglia,‡[c] Chiara Gabbiani,[a] Ida Landini,[d] Tania Gamberi,[b] Dolores Fregona,[e] Maria Agostina Cinellu,[f] Stefania Nobili,[d] Enrico Mini,[d] Luca Bini,[c] Pietro Amedeo Modesti,[g] Alessandra Modesti*[b] and Luigi Messori*[a]

Received 23rd September 2011, Accepted 2nd November 2011
DOI: 10.1039/c1mb05386h

Cytotoxic gold compounds hold today great promise as new pharmacological agents for treatment of human ovarian carcinoma; yet, their mode of action is still largely unknown. To shed light on the underlying molecular mechanisms, we performed 2D-DIGE analysis to identify differential protein expression in a cisplatin-sensitive human ovarian cancer cell line (A2780/S) following treatment with two representative gold(III) complexes that are known to be potent antiproliferative agents, namely AuL12 and Au_2Phen. Software analysis using DeCyder was performed and few differentially expressed protein spots were visualized between the three examined settings after 24 h exposure to the cytotoxic compounds, implying that cellular damage at least during the early phases of exposure is quite limited and selective, reflecting the attempts of the cell to repair damage and to survive the insult. The potential of novel proteomic methods to disclose mechanistic details of cytotoxic metallodrugs is herein further highlighted. Different patterns of proteomic changes were highlighted for the two metallodrugs with only a few perturbed protein spots in common. Using MALDI-TOF MS and ESI-Ion trap MS/MS, several differentially expressed proteins were identified. Two of these were validated by western blotting: Ubiquilin-1, responsible for inhibiting degradation of proteins such as p53 and NAP1L1, a candidate marker identified in primary tumors. Ubiquilin-1 resulted over-expressed following both treatments and NAP1L1 was down-expressed in AuL12-treated cells in comparison with control and with Au_2Phen-treated cells. In conclusion, we performed a comprehensive analysis of proteins regulated by AuL12 and Au_2Phen, providing a useful insight into their mechanisms of action.

Introduction

Ovarian cancer is the second among gynecological cancers in number of new cases and the first among gynecological cancers in rate of deaths in Western countries.[1] It is characterized by few and nonspecific early symptoms, typically showing up only in a rather advanced stage, which explains the poor survival of ovarian cancer patients (*i.e.* overall 5 year survival is around 45%).[2] Platinum-based chemotherapy, such as that using cisplatin, is the election treatment for human ovarian cancer. However, despite the relevant contribution of cisplatin in ameliorating the quality of life and the overall survival of cancer patients, the occurrence of intrinsic or acquired tumor chemoresistance remains a major determinant of chemotherapy failure and of unfavorable clinical outcome.[3,4] Because of cisplatin resistance, several new platinum and non-platinum metal compounds were prepared, characterized and evaluated pharmacologically as alternative chemotherapeutic agents for ovarian carcinoma treatment.[5] In recent years, research has increasingly focused on cytotoxic gold compounds as drug candidates.[6] In fact, gold(III) complexes display the same electronic configuration (d8) and similar structural and reactivity features to platinum(II) complexes[7] (in particular a strong preference for square-planar geometry and a rather favourable kinetic profile) but the respective mechanisms appear to be drastically different. A number of gold(III) complexes

[a] *Department of Chemistry, University of Florence, via della Lastruccia 3, 50019 Sesto Fiorentino, Italy. E-mail: luigi.messori@unifi.it; Fax: +39 055 4573385; Tel: +39 055 4573388*
[b] *Department of Biochemical Sciences, University of Florence, viale G. Morgagni, 50, 50134 Firenze, Italy. E-mail: modesti@scibio.unifi.it; Fax: +39 055-4598905; Tel: +39 055-5498311*
[c] *Department of Molecular Biology, University of Siena, via Fiorentina, 1, 53100 Siena, Italy*
[d] *Department of Pharmacology, University of Florence, viale Pieraccini 6, 50139 Firenze, Italy*
[e] *Department of Chemical Sciences, University of Padova, via Marzolo 1, 35131 Padova, Italy*
[f] *Department of Chemistry, University of Sassari, via Vienna 2, 07100 Sassari, Italy*
[g] *Department of Medical and Surgical Critical Care, University of Florence, largo Brambilla, 3, 50100 Firenze, Italy*
† Presented, in part, at the 6th Annual National Conference of the Italian Proteomics Association held in Turin 21st–24th June 2011.
‡ These authors equally contributed to this work.

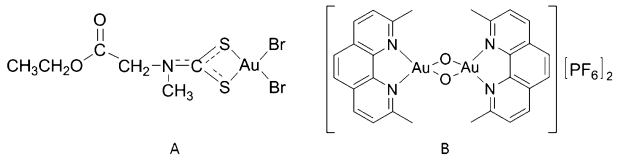

Fig. 1 AuL12 (A) and Au_2phen (B).

were found to possess promising pharmacological profiles *in vitro* and in some cases also *in vivo*.[8,9]

The present investigation is focused on AuL12, a gold(III) dithiocarbamate compound that was reported to be particularly effective both *in vitro* and *in vivo*,[10] and Au_2Phen, a binuclear gold(III) complex that manifested outstanding properties *in vitro* when challenged against a large panel of human tumor cell lines.[11] Fig. 1 shows the chemical structure of AuL12 and Au_2Phen.

Remarkably, AuL12 shows higher anticancer activity than cisplatin itself toward all the murine tumor models, inducing up to 80% inhibition of tumor growth. In addition, it shows low acute toxicity levels and reduced nephrotoxicity.[10]

The application of wide approaches, such as proteomics, might lead to further progress in understanding the mechanisms of action of gold compounds. Proteomic approaches were recently exploited to investigate the mode of action of anticancer metallodrugs.[12–14]

Moreover, the introduction of fluorescence-based methodologies in the 2-DE field has provided a substantial advantage in proteomic investigations. 2-D DIGE is characterized by a high sensitivity, a wide linear dynamic range for quantitative accuracy and when utilizing a sample multiplexing strategy and gel coordination *via* an internal standard, a direct quantitative evaluation of changes, as well as minimization of experimental variation. Accordingly, DIGE analysis generates highly accurate data with reliable biological significance.

In our previous proteomic works we showed that various cytotoxic gold compounds produce their antiproliferative effects through a variety of molecular mechanisms and that a number of distinct protein targets are likely involved.[15] In particular, we analyzed proteomic alterations induced by Auranofin and Auoxo6 in a human ovarian cancer cisplatin-sensitive cell line (A2780/S) and in its parental resistant cell line (A2780/R). In both cell lines Auranofin and Auoxo6 caused relatively modest changes in protein expression in comparison with controls. Some of the affected proteins are primarily involved in intracellular redox homeostasis, implying that cell damage is probably the consequence of severe oxidative stress; pair wise, proteins that are biomarkers of apoptosis were found to be greatly perturbed.

We report here the results of a DIGE proteomic study on the cellular effects of two additional cytotoxic gold compounds, AuL12 and Au_2Phen, by comparing the proteomic profiles of A2780/S cells treated with those of controls. Applying 2-D DIGE with dedicated software analysis, few differentially expressed protein spots were visualized between the control and the two drug treatments examined, indicating that the two different gold compounds cause different proteomic modifications. Successive mass spectrometry application, MALDI-TOF MS and ESI-Ion trap MS/MS allowed the identification of several differentially expressed proteins and for the most interesting candidates, the proteomic analysis was validated by western blotting. Detailed functional analysis of the altered proteins provides valuable insight into the possible biochemical mechanisms that are elicited by AuL12 and Au_2Phen.

Results and discussion

Antiproliferative effects of AuL12 and Au_2Phen toward A2780 cells

Cytotoxic effects of AuL12 and Au_2Phen against the above reported human ovarian carcinoma cell lines, A2780/S and A2780/R, were determined according to the procedure of Skehan.[16] After 72 h of exposure to the two compounds a relevant cytotoxic activity was observed. CI_{50} values fell in the low μM range (Table 1) for both compounds. In particular, the two compounds were more active than cisplatin against the resistant cell line and Au_2Phen also against the sensitive cell line. Cross-resistance ratios (*r*) of the study compounds were markedly lower (*i.e.* 1.3 and 4.1 for AuL12 and Au_2Phen, respectively) than that of cisplatin (16.9) (Table 1).

Analysis of 2-D DIGE images of A2780/S gold-treated and untreated cells

To analyze in detail protein expression modifications induced by the two gold compounds, quantitative proteomic analysis of A2780/S gold-treated and untreated cells was performed according to high-sensitive 2-D DIGE. A2780/S cells were incubated for 24 h with AuL12 and Au_2Phen at a concentration corresponding to their 72 h exposure CI_{50} values (4.0 and 0.8 μM, respectively) and protein extracts were subsequently prepared for DIGE analysis, as previously reported in "Experimental".

Resulting Cydye™-stained gels were analyzed using DeCyder software. For each condition, triplicate biological repeats were obtained and reverse labelled by Cy3 and Cy5, while the Cy2 dye was used for the internal standard. Generated from an equal combination of all the samples tested in the same experiment, the standard allows a proper quantitative comparison of proteomic variations with statistical confidence, as described under "Experimental". A total of 9 samples labelled with Cy3 and Cy5 were run in five gels along with a pooled standard labelled with Cy2

Table 1 Antiproliferative activity of AuL12, Au_2Phen and cisplatin against A2780 ovarian carcinoma human cell lines, either sensitive (A2780/S) or resistant (A2780/R) to cisplatin

	A2780/S CI_{50} (μM) ± SD	A2780/R CI_{50} (μM) ± SD
AuL_{12}		
Mean	4.0 ± 1.0	5.2 ± 1.3
R		*1.3*
Au_2Phen		
Mean	0.8 ± 0.1	3.2 ± 1.6
R		*4.1*
Cisplatin		
Mean	1.6 ± 0.5	26.5 ± 3.1
R		*16.9*

The experiment was performed in triplicate; *R*, cross-resistance ratios; SD, standard deviation.

Table 2 Experimental design for 2-D DIGE proteome profiling. Three biological replicate samples for each group (C1–C2–C3: control replicates; A1–A2–A3: AuL12 samples; B1–B2–B3: Au_2Phen samples) were used and labelled with Cy3 or Cy5. Each gel contained the pooled standard (equal aliquots of all the samples in all groups) and two other subject samples. Thus, the 14 samples were analyzed by running five gels. (For detailed description refer to "Experimental.")

Gel	Cy3	Cy5	Cy2
1	C1	B1	Pooled internal standard sample
2	A1	C2	Pooled internal standard sample
3	C3	A2	Pooled internal standard sample
4	B2	A3	Pooled internal standard sample
5	B3		Pooled internal standard sample

giving a total of 14 images. For samples resolved in the same gel, quantification of the proteins was performed first by dividing the Cy3 or Cy5 signals by the Cy2 intensities, and then these intragel ratios were compared with the ratios from other gels. Thus, for a given protein, the normalized abundance ratios from all 9 samples can be intercompared in an five-gel experiment as the protein spot intensity in every gel is normalized to the same internal standard. To compute the fold changes in protein expression between the groups and their statistical significance, once the standardized abundance ratios for spots in every gel were computed, the corresponding Cy3 and Cy5 spot maps for 9 samples were grouped according to the group description as described in the experimental design (Table 2).

According to the DeCyder software analysis, about 2500 protein spots were constantly detected in each gel and quantified, normalized and inter-gel-matched. Due to the CyDye DIGE Fluor detection limit and the CyDye linear response in protein concentrations over five orders of magnitude, 26 protein spots had significant differences occurring between the untreated control cells and the two different settings of drug-treated cells. In Fig. 2, a representative 2-D DIGE spot map of AuL12-treated A2780/S cells is reported, showing all the differences found between the two different drug-treatments and the control. Protein expression changes were considered significant when their quantity decreased or increased by at least 1.3-fold. In order to find proteic differences characteristics of each gold-compound we performed a univariate analysis (AuL12 *vs.* control; Au_2Phen *vs.* control) with a two tailed Student's *t*-test, $p \leq 0.05$ and was statistically supported by a one-way ANOVA (*p*-value $<$ 0.05). In order to find proteic differences in common between the two treatments, we performed a one-way ANOVA, $p \leq 0.05$.

Remarkably, both AuL12 and Au_2Phen treatments caused small modifications of protein expression profiles. Only a limited number of protein spots manifested appreciable down- or up-regulation. According to our statistics, among the detected biological variations, 8 protein spots (5 down-regulated and 3 up-regulated) and 10 protein spots (2 down-regulated and 8 up-regulated) had significantly changed volume values after AuL12 and Au_2Phen treatment, respectively, as compared to the

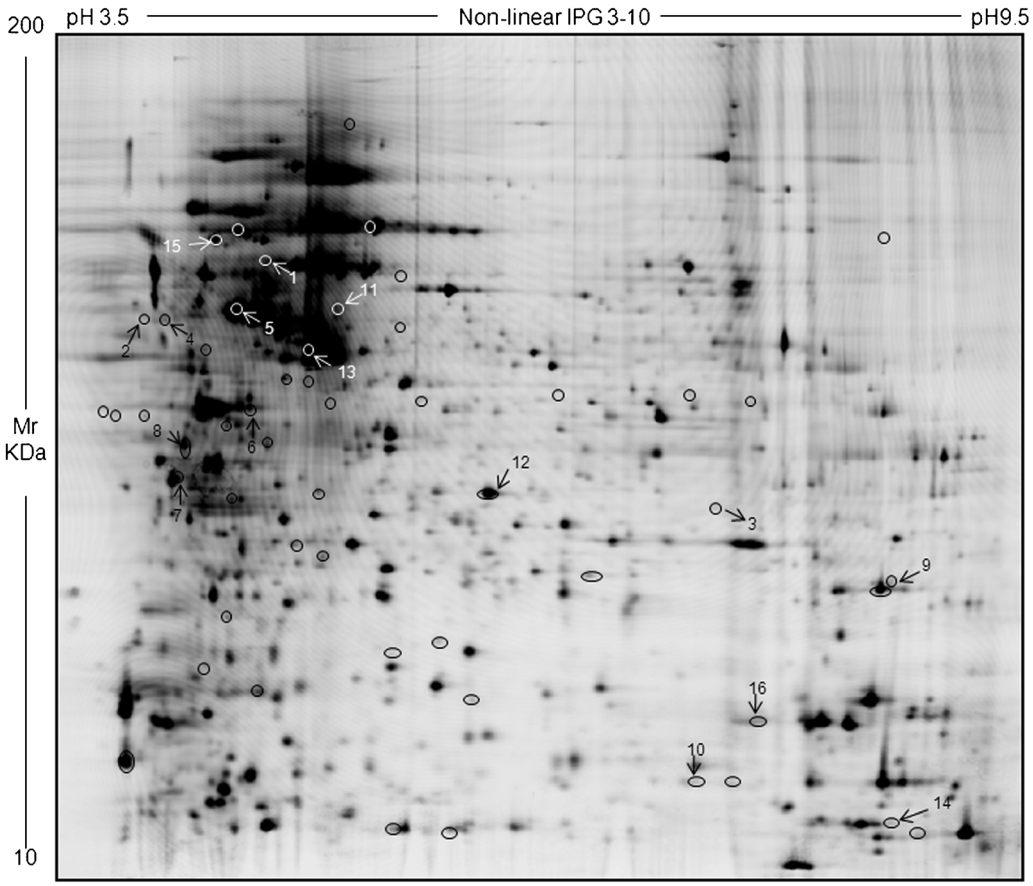

Fig. 2 Representative Cy3-labeled spot map of A2780/S cells treated for 24 h with AuL12. All the detected differences between the control cells and the two drug-tested conditions are visualized by black circles. We used white circles when the image was too dark for black ones. For MS-identified protein spots, the spot numbers match those listed in Tables 3 and 4.

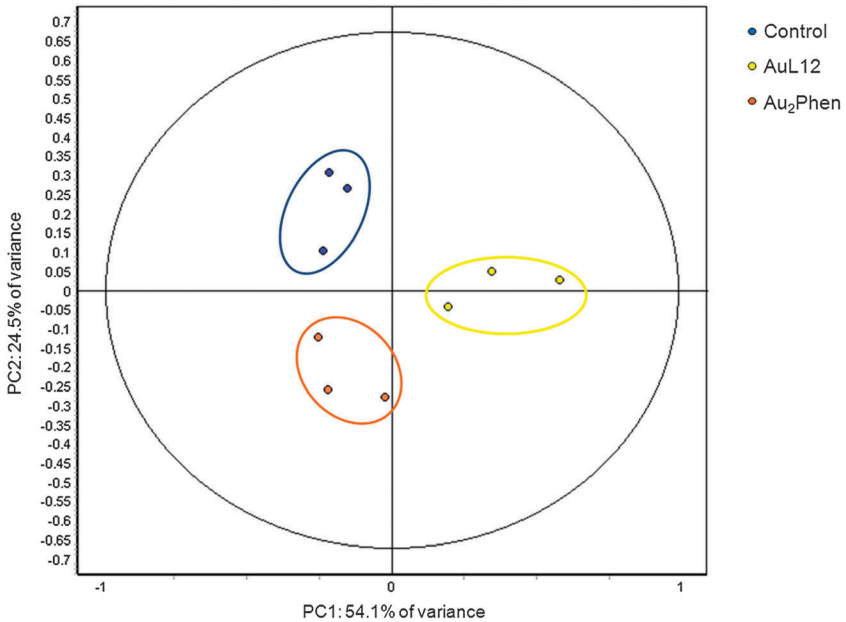

Fig. 3 The protein expression profiles of experimental groups were visualized in two-dimensional Euclidian space by using the extended data analysis module of DeCyder software as described under "Experimental". PCA distinctly clustered the 9 individual samples into three experimental groups corresponding to the three experimental conditions (Control; AuL12 and Au_2phen).

control group. In addition, 8 protein spots (1 down-regulated and 7 up-regulated) were detected as differentially expressed after both treatments, when compared with control cells. The locations of these protein spots are marked with black and white circles in the representative gel shown in Fig. 2.

Principal component analysis (PCA)

In addition to univariate analysis, multivariate analyses were performed to explore categories of differential protein expression. To examine relationships existing between the three tested conditions and to corroborate the biological validity of the BVA results (see "Experimental" for analyses details), acquired data were processed in an unsupervised manner, using multivariate analysis methods according to the DeCyder EDA module. Protein spots included in the analyses were those present in 80% of the spot maps and with expression variation of at least 1.3-fold at the 95th confidence level (one-way ANOVA, $p \leq 0.05$). The Principal Component Analysis (PCA) revealed distinct expression profiles between drug-treated and untreated A2780/S cells (Fig. 3). PCA demonstrated consistent reproducibility between the biological triplicates, as spot maps properly segregated into three experimental groups (encircled by different colours) that are clearly separated from each other in the PCA plot. The first principal component (PC1) accounted for 54.1% of the variance in the data, while the second principal component (PC2) accounted for an additional 24.5% of the variation.

Proteomic profiles of treated and control cells

Interesting spots were excised from preparative SyproRuby stained 2-DE gels loaded with 800 μg of total proteins for protein identification by tryptic in-gel digestion and MALDI-TOF MS and/or LC-MS/MS analysis. Following a Mascot engine search, using the acquired MS data, 16 spots were identified. Not all spots could be identified because of the relatively low protein concentrations and MS sensitivity limitations. Positions of the identified spots are indicated by numbers in the representative gels

Table 3 Mass spectrometry identified proteins

			MASCOT search results			Fold change[e]	
Spot no	AC[a]	Protein name	No. of matched peptide[b]	Sequence coverage%[c]	Score[d]	AuL12/ control	Au_2Phen/ control
1	P61978	Heterogeneous nuclear ribonucleoprotein K	10	24	89		1.63
2	Q14257	Reticulocalbin-2	8	34	135		1.68
3	Q9NQR4	Omega-amidase NIT2	11	41	176		1.42
4	P55209	Nucleosome assembly protein 1-like 1	6	22	103	−1.54	
5	P07437	Tubulin beta chain	20	43	224	−1.40	
6	Q9Y3F4	Serine–threonine kinase receptor-associated protein	8	32	121	−1.35	
7	P24534/P62258	Mix Elongation factor 1-β/14-3-3	7/9	46/31	90/74	1.45	
8	P12004	Proliferating cell nuclear antigen	11	47	132	−1.45	

[a] Swiss-Prot/TrEMBL accession number. [b] Number of peptide masses matching the top hit from Ms-Fit PMF. [c] Percentage of amino acid sequence coverage of matched peptides in the identified proteins. [d] MASCOTscore (Matrix Science, London, UK; http://www.matrixscience.com). [e] Fold change (AuL12 *vs.* control and Au_2Phen *vs.* control) was calculated dividing %V from AuL12 or Au_2Phen by the %V from control.

Table 4 Mass spectrometry identified proteins in common between the two treatments

			MASCOT search results				
Spot no	AC[a]	Protein name	No. of matched peptide[b]	Sequence coverage%[c]	Score[d]	Fold change[e]	One-way-ANOVA
9	P23919	Thymidylate kinase	10	44	122	1.41	0.042
10	P49773	Histidine triad nucleotide-binding protein 1	7	65	114	1.33	0.030
11	P28838	Cytosol aminopeptidase	2	TIQVDNTDAEGR	45/33	−1.35	0.044
12	P63104	14-3-3 protein zeta/delta	6	SVTEQGAELSNEER	65/32	1.44	0.046
13	P60709	Actin, cytoplasmic 1	11	21	130	1.61	0.041
14	P14174	Macrophage migration inhibitory factor	2	PMFIVNTNVPR	48/32	1.39	0.025
15	Q9UMX0	Ubiquilin-1	4	FQQQLEQLSAMGFLNR	83/31	1.37	0.030
16	P62937	Peptidyl-prolyl *cis–trans* isomerase A	8	56	120	1.49	0.032

[a] Swiss-Prot/TrEMBL or NCBInr accession number. [b] Number of peptide masses matching the top hit from Ms-Fit PMF. [c] Percentage of amino acid sequence coverage of matched peptides in the identified proteins. Reported sequence peptide correspond to one of those resulted from MS/MS analysis after ambiguous identifications by MALDI-ToF in that spot. [d] MASCOTscore (Matrix Science, London, UK; http://www.matrixscience.com). [e] Fold change [Au_2Phen + AuL12] *vs.* [Control] was calculated dividing %V from AuL12 and Au_2Phen by the %V from control.

shown in Fig. 2. A list of the up- and down-regulated proteins is given in Tables 3 and 4. Tables report all identified proteins, protein name, NCBI database accession number, Mascot score, peptide matched, sequence coverage and statistical analysis (fold change ± 1.3 and p-value < 0.05). In particular Table 3 indicates proteins found as differences following a single treatment, while Table 4 indicates proteins found as differences in common between the two treatments. A group of 4 protein spots (4, 5, 6, 8) shows a significant down-regulation in AuL12-treated cells *versus* controls. One protein spot (7) shows an increase in the intensity level. The volume of 3 protein spots (1, 2, 3) was significantly up-regulated in the Au_2Phen-treated cells with a p-value ranging between 0.05 and 0.005 when compared with the control group. Among the identified protein spots we found 1 spot down-expressed in both treatments (11) and 7 proteins up-regulated (9, 10, 12, 13, 14, 15, 16).

Proteins over-expressed in Au_2Phen treated cells

We identified by mass spectrometry Heterogeneous nuclear ribonucleoprotein K (Spot 1) as up-regulated in Au_2Phen treated cells. This protein belongs to the family of hnRNPs, RNA binding proteins that appear to influence pre-mRNA processing and mRNA metabolism and transport. This protein is located in the nucleoplasm and it seems to have a role during the cell cycle progression. Hope and Murray defined the expression profile of Heterogeneous nuclear ribonucleoproteins in colorectal cancer and they showed that there are significant alterations in both expression and subcellular localization of individual heterogeneous nuclear ribonucleoproteins in this type of tumor.[17] We also found an over-expression for Reticulocalbin-2 (RCN) (Spot 2). This protein does not have known function but its expression may be related to differential diagnoses of some types of tumors, although an extensive distribution of RCN has been demonstrated in various normal organs.[18] We found an over-expression of omega-amidase NIT2 (Spot 3), largely distributed in nature, that has been suggested to be a tumor suppressor protein. Its role is to remove potentially toxic intermediates by converting α-ketoglutaramate and α-ketosuccinamate to biologically useful α-ketoglutarate and oxaloacetate, respectively. Some authors report the crucial role of NIT2 in nitrogen and sulfur metabolism, and the possible link of NIT2 to cancer biology.[19]

Proteins over-expressed in AuL12 treated cells

In one spot (Spot 7), showing a significant positive correlation with AuL12 treatment, we identify by mass spectrometry two proteins: the Elongation factor 1-β and the 14-3-3 protein epsilon. The first protein is involved in the biosynthesis of proteins from mRNA molecules. The second is an adapter protein implicated in regulation of a large spectrum of both general and specialized signaling pathways.[20]

Proteins down-expressed in AuL12 treated cells

We observed a reduced expression pattern of Nucleosome assembly protein 1-like 1 (NAP1L1) (Spot 4). It is involved in modulating chromatin formation and it contributes to regulation of cell proliferation. It is a candidate marker identified by transcriptional profiling in primary tumors and metastases and in carcinomas. The ability to determine the malignant potential of these tumors and their propensity to metastasize provides a biological rationale for the management of carcinoids and may have prognostic utility.[21] Among proteins down-expressed in AuL12 treated cells we found tubulin beta chain (TBB5) (Spot 5). It is a protein associated with chemotherapeutic responses. In chemoresistant tissues, tubulin α-1A chain was over-expressed. This protein may be useful as predictive of chemoresistance.[22] Also serine–threonine kinase receptor-associated protein (STRAP) (Spot 6) has been found down-expressed. It plays an essential role in spliceosomal snRNP assembly in the cytoplasm and it is required for pre-mRNA splicing in the nucleus. A correlation between STRAP over-expression and various cancers has been identified and it is becoming clear that STRAP regulates several distinct cellular processes and modulates multiple signaling pathways.[23]

The proliferating cell nuclear antigen (PCNA) (Spot 8) is down-expressed after AuL12 treatment. This protein is involved in control of eukaryotic DNA replication, inducing a robust stimulatory effect on DNApolymerase activity.[24]

Proteins over-expressed following both treatments

Thymidylate kinase (Spot 9) is one of the essential enzymes involved in the pyrimidine synthesis. Romain *et al.* investigated its relationship with breast cancer. They measured thymidine kinase (TK), thymidylate synthase (TS) and thymidylate kinase

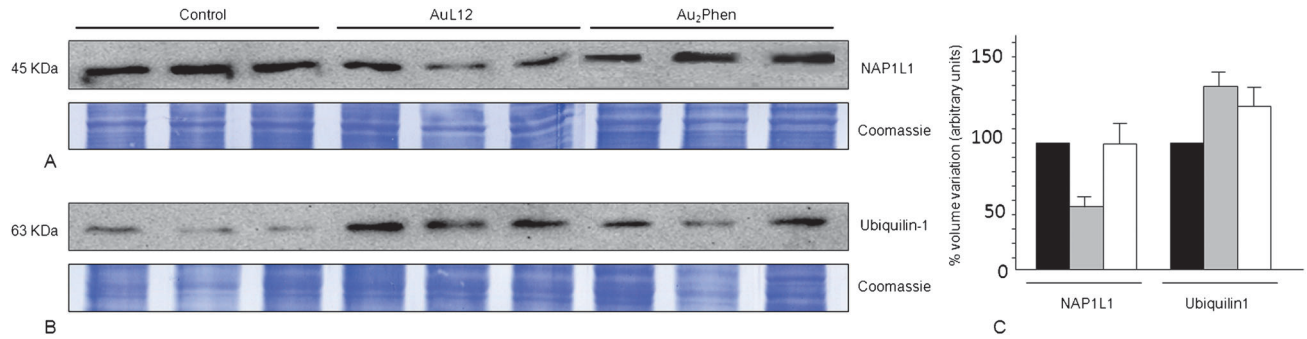

Fig. 4 Validation of proteomic results by western blot analysis. Western blots were probed with antibodies against NAP1L1 and Ubiquilin-1 proteins identified by proteomic screening. The intensity of immunostained bands was normalized with the total protein intensities measured from the same blot stained with Coomassie brilliant blue (in panel A and panel B a representative band of the lane is reported). (A) AuL12-induced reduced expression of NAP1L1 after 24 h of treatment. (B) AuL12-induced and Au_2Phen-induced increased expression of Ubiquilin-1 after 24 h of treatment. (C) Histograms representing NAP1L1 and Ubiquilin-1 protein expression variation. The two-tailed non-paired Student's *t*-test was performed using ORIGIN 6.0 ($p < 0.05$).

(TMK). Among the enzymes analyzed, only TK demonstrated a strong correlation with the most aggressive tumors. In contrast, TS and TMK were not associated with prognosis and metastasis formation.[25] We found histidine triad nucleotide-binding protein 1 (Hint1) (Spot 10). It is a member of the evolutionarily conserved family of histidine triad proteins that acts, with a poorly defined molecular mechanisms, as a haplo-insufficient tumor suppressor. Consistent with a tumor suppressor function, in the human non-small cell lung cancer cell line NCI-H522, a reduced expression of Hint1, was observed and its re-introduction resulted in cell growth inhibition and reduced tumorigenicity. Moreover Hint1 is involved in regulation of apoptotic pathways by inducing an up-regulation of p53 expression.[26] We found 14-3-3 Protein Zeta/delta (Spot 12) as over-expressed: it belongs to the 14-3-3 proteins family that have been shown to regulate many important cellular mechanisms. However, the expression of 14-3-3 isoforms still remains unknown.[27] We found an over-expression of peptidyl-prolyl *cis–trans* isomerase A (PPI1A or cyclophilin A) (Spot 16); this protein belongs to the family of PPIases whose activity is to accelerate the proteins folding. PPI1A has been reported to be upregulated in diverse human cancers and its over-expression induces resistance to chemotherapeutic agents such as cisplatin in cancer cells.[28] Also the macrophage migration inhibitory factor (MIF) (Spot 14) has been found to be over-expressed. It is a pro-inflammatory cytokine involved in the innate immune response. The expression of MIF at sites of inflammation suggests a role as mediator in regulating the function of macrophages in host defense.[29] We found an over-expression of Ubiquilin-1 (Spot 15), responsible for the inhibition of proteasome-mediated protein degradation. In particular, Patel *et al.* observe that Ubiquilin-1 is responsible for inhibiting proteasome-mediated protein degradation in a range of proteins, such as p53, cyclin A and IkB.[30]

Protein down-expressed in both treatments

The only protein identified whose expression resulted down-regulated following both treatments is the cytosol aminopeptidase (Spot 11). It is involved in processing and regular proteins turnover. This protein catalyzes the removal of unsubstituted N-terminal amino acids from various peptides and it is involved in the proteasome/ubiquitin pathway. Its down-expression, inhibiting protein turnover, could result in cell apoptosis and it could represent a novel therapeutic approach.[31]

Validation of differentially expressed proteins by immunoblotting

To validate the DIGE/MS-obtained results, as well as to further evaluate the nature and importance of some of the identified proteins that changed expression after drug treatment, mono-dimensional (1D) western blotting analyses were performed. Proteins with identified expression changes were selected for immunoblotting analysis according to their known or supposed involvement in the biochemical pathways affected by the evaluated drugs, based on the available literature. For these analyses, a new experiment was performed on A2780/S cells either untreated or treated for 24 h with AuL12 and Au_2Phen. Two proteins, Ubiquilin-1 and NAP1L1, were validated by western blotting. As shown in Fig. 4, NAP1L1 is down-expressed in AuL12-treated cells in comparison with control and in comparison with Au_2Phen-treated cells. Ubiquilin-1 resulted over-expressed following both treatments in comparison with control. The protein expression-fold changes are consistent with the reported 2-D DIGE results.

Experimental

Materials and reagents

Au_2Phen was synthesized as described by Cinellu *et al.*[11] The gold(III) complex AuL12 was synthesized and purified as previously described.[32] All other chemicals were of analytical grade. RPMI 1640 cell culture medium, fetal calf serum (FCS) and phosphate-buffered saline were obtained from Celbio (Milan, Italy); sulforhodamine B (SRB) was obtained from Sigma (Milan, Italy).

Cell lines and cell culture

The human ovarian carcinoma cell line sensitive to cisplatin (A2780/S) and its cisplatin-resistant cell subline (A2780/R) were used for cytotoxicity studies and the A2780/S subline for proteomic studies. Cell lines were maintained in RPMI1640

medium supplemented with 10% of FCS and antibiotics at 37 °C in a 5% CO_2 atmosphere and subcultured twice weekly.

Cell growth inhibition studies

The cytotoxic activity of AuL12 and Au_2Phen was evaluated against the A2780/S and A2780/R cell lines according to the procedure described by Skehan.[16] Both compounds were diluted in DMSO as stock solutions (10 mM). Exponentially growing cells were seeded in 96-well microplates at a density of 5×10^3 cells per well. After cell inoculation, the microtitre plates were incubated under standard culture conditions (37 °C, 5% CO_2, 95% air and 100% relative humidity) for 24 h prior to the addition of study compounds. After 24 h, the medium was removed and replaced with fresh medium containing drug concentrations ranging from 0.003 to 100 μM for a continuous exposure of 72 h for both compounds tested. For comparison purposes the cytotoxic activity of cisplatin against the A2780/S and A2780/R cells, measured under the same experimental conditions, was also determined. Then cells were fixed with 100 μL of ice-cold 10% trichloroacetic acid (TCA) for 60 min at 4 °C, rinsed 6 times with water and air-dried. Fixed cells were stained with 50 μL of sulforhodamine B (SRB) solution (0.4% SRB/0.1% acetic acid), rinsed with 0.1% acetic acid and air-dried. At the end of the staining period, SRB was dissolved in 150 μL of 10 mM Tris–HCl solution (pH 10.5) for 10 min in a gyratory shaker. Optical density was read in a microplate reader interfaced with the software Microplate Manager/PV version 4.0 (Bio-Rad Laboratories, Milan, Italy) at 540 nm. The CI_{50} drug concentration resulting in a 50% reduction in the net protein content (as measured by SRB staining) in drug-treated cells as compared to untreated control cells was determined after 72 h of drug exposure. The reported CI_{50} data represent the mean of at least three independent experiments.

Sample preparation and labelling with CyDyes

Whole protein extracts were obtained from A2780/S cells and A2780/S cells treated with AuL12 and Au_2Phen. Briefly, cells were seeded in tissue-culture plates at 5×10^4 cells mL^{-1} (total volume 30 mL) and incubated overnight, then exposed to concentrations of the study compounds equal to 72 h exposure CI_{50} values for 24 h. At the end of incubation cells were washed with phosphate-buffered saline, then were scraped in RIPA buffer [50 mM Tris–HCl pH 7.0, 1% NP-40, 150 mM NaCl, 2 mM ethylene glycol bis(2-aminoethyl ether)tetraacetic acid, 100 mM NaF] containing a cocktail of protease inhibitors (Sigma). Cells were sonicated (10 s) and protein extracts were clarified by centrifugation at 8000*g* for 10 min. Proteins were precipitated following a chloroform/methanol protocol and pellets obtained were then resuspended with lysis DIGE buffer (7 M urea, 2 M thiourea, 4% (w/v) CHAPS and 25 mM Tris). Protein concentration was estimated by Bradford's assay[33] and as the protein concentration was more than 5 μg μL^{-1} for all the samples, we proceed with the fluorescence dye labelling. Minimal protein labeling for 2-D DIGE was performed according to the manufacturer's instructions (GE Healthcare). It was prepared as an internal standard resulting from pooling aliquots of the nine experimental samples, which was labelled with the fluorescent cyanine dye Cy2. Samples from A2780/S cells untreated and treated with AuL12 or Au_2Phen were labelled with Cy3 or Cy5 cyanine dyes by the addition of 480 pmol of CyDye in 1.2 μL of anhydrous *N*,*N*-dimethylformamide per 60 μg of protein. An alternate dye labelling was used such that the three samples for any condition were variously labelled with Cy3 or Cy5 to avoid any dye-specific staining bias. Labelling incubation was performed on ice in the dark for 30 min; then the reaction was stopped by the addition of 10 mM lysine on ice for 10 minutes. Cy3 and Cy5 quenched samples, according to the experimental design (Table 1), were mixed together with an aliquot of Cy2 labelled standard and an equal volume of 2× DIGE buffer (7 M urea, 2 M thiourea, 4% (w/v) CHAPS and 2% (w/v) DTE). Previous to isoelectric focusing (IEF), the total volume was increased to 450 μL with 1× DIGE rehydration solution (7 M urea, 2 M thiourea, 4% (w/v) CHAPS and 1% (w/v) DTE) and loaded on commercial nonlinear wide-range immobilized pH gradients (IPGs; pH 3.0–10; 24 cm long IPG strips; Biorad).

DIGE two dimensional gel electrophoresis

The first dimension (IEF) was achieved using an Ettan IPGphor™ system (GE Healthcare). Runs were performed at 16 °C in the dark, until a total of 80 000 V h^{-1} were reached. Focused strips were equilibrated in 6 M urea, 2% (w/v) SDS, 2% (w/v) DTE, 30% (v/v) glycerol and 0.05 M Tris–HCl pH 6.8 for 12 min and subsequently for 5 min in the same urea/SDS/Tris–HCl buffer solution where DTT was substituted with 2.5% iodoacetamide. The second dimension was carried out at 15 °C on 9–16% polyacrylamide linear gradient gels (24 cm × 20 cm × 1 mm) at 17 W/gel constant Watt using an Ettan Dalt II system (GE Healthcare). Runs were performed until the dye front reached the bottom of the gel, in accordance with Hochstrasser *et al.*[34] All electrophoresis procedures were performed in the dark.

Image analysis

DIGE gel images were acquired by the Typhoon 9400 imager (GE Healthcare). All gels were scanned at 100 μm resolution. Data analysis was carried out using DeCyder 2D v7.0 Software (GE Healthcare). A total of 14 gel images consisting of three biological replicate images from A2780/S cells untreated, three replicates from A2780/S cells treated with AuL12, three replicates from A2780/S cells treated with Au_2Phen and five replicates from the internal standards were processed. Quantification of spot intensity data was performed by the differential in-gel analysis (DIA) module of DeCyder software: all spots from each gel were detected and normalized volume ratios for each protein were calculated by using the individual signal of pooled-sample Cy2-labelled as an internal standard. The biological variation analysis (BVA) module allowed samples to be inter-compared along with the experimental design by the univariate analysis across the five gels. Protein spot variation was considered significant if the normalized spot volume showed at least ±1.3 fold change and a p-value < 0.05 (two tailed Student's t-test). Protein spots that satisfy these parameters were signed as protein of interest. We also performed a multivariate analyses, using the extended data analysis (EDA) module, to

highlight proteins with similar expression patterns among the three experimental conditions, p-value < 0.05 (one way ANOVA). Relationships among spot maps were visualized by performing a principal component analysis (PCA) according to the intensity values of protein spots marked as protein of interest in the BVA module. All spot maps were distributed in a two-dimensional space, along with the first two principal components, PC_1 and PC_2, that represented the largest sources of variation in the experimental data set.

Mass spectrometry MALDI-TOF and LC-ESI/MS-MS

MS-preparative IPG strips (24 cm non-linear pH 3–10, Biorad) were rehydrated with 450 μL of 1× DIGE rehydration solution and 2% v/v Pharmalyte pH 3–10 (GE Healthcare), for 12 h at room temperature using a re-swelling tray (GE Healthcare). For MS-preparative gels, 800 μg of total proteins, obtained by pooling all our conditions, were loaded on both cathodic and anodic ends of the IPGphor Cup Loading Strip Holders (GE Healthcare). Runs were performed at 16 °C, until a total of 110 000 V h^{-1} for strip were reached. Strip equilibration and second dimension were performed as described above for the DIGE runs. MS-preparative gels were stained with SYPRO Ruby (Biorad) according to the manufacturer's instructions. The internal surface of the inner low fluorescence plate was previously treated with Bind-Silane (γ-methacryloxypropyltrimethoxysilane; LKB-Produkter AB, Brommo, Sweden), air dried for 1 h to covalently attach polyacrylamide gels subjected to SYPRO Ruby staining and automatic cutting by Ettan Spot Picker (GE Healthcare). Protein identification was mainly carried out by peptide mass fingerprinting (PMF) on an Ettan MALDI-ToF Pro mass spectrometer (GE Healthcare) as previously described.[35–37] After visualization by an SYPRO Ruby staining protocol, all the spots of interest were mechanically excised, destained in 2.5 mM ammonium bicarbonate and 50% acetonitrile and finally dehydrated in acetonitrile. They were then rehydrated in trypsin solution and in-gel protein digestion was performed by overnight incubation at 37 °C. Each protein digest (0.75 μL) was spotted onto the MALDI target and allowed to air dry. Then 0.75 μL of matrix solution (saturated solution of α-cyano-4-hydroxycinnamic acid in 50% (v/v) acetonitrile and 0.5% (v/v) TFA) was applied to the sample which was then dried again. Mass spectra were acquired automatically using the Ettan MALDI Evaluation software (GE Healthcare). Spectra were internally calibrated using the autoproteolysis peptides of trypsin (842.51 and 2211.10 Da). PMF searching was carried out in UniProtKB databases using MASCOT (Matrix Science Ltd, London, UK, http://www.matrixscience.com). Taxonomy was limited to Homo sapiens, a mass tolerance of 100 ppm was allowed and the number of accepted missed cleavage sites was set to one. Alkylation of cysteine by carbamidomethylation was considered a fixed modification, while oxidation of methionine was considered as a possible modification. The criteria used to accept identifications included the extent of sequence coverage, the number of matched peptides and a probabilistic score. Tryptic digests that did not produce MALDI-TOF unambiguous identifications were subsequently subjected to peptide sequencing on a nanoscale LC-ESI/MS-MS, as described in detail by Meiring *et al*.[37] All the analyses were carried out on an LC-MS system consisting of a PHOENIX 40 (ThermoQuest Ltd., Hemel Hempstead, UK) and an LCQ DECA IonTrap mass spectrometer (Finnigan, SanJose, CA, USA). The peptides, after a manual injection (5 μL) in a six-port valve, were trapped in a C18 trapping column (20 mm × 100 μm ID × 360 μm OD, Nanoseparations, Nieuwkoop, NL) using a 100% solvent A (HPLC grade water + 0.1% (v/v) formic acid) under a flow rate of 5 μL min^{-1} for 10 min. A linear gradient up to 60% solvent B (acetonitrile + 0.1% (v/v) formic acid) for 30 min was used for analytical separation and, using a pre-column splitter restrictor, we obtained a column flow rate of 100–125 nL min^{-1} on a C18 analytical column (30 cm × 50 μm ID × 360 μm OD, Nanoseparations). Before the injection of the next sample, both the trapping and analytical column were equilibrated for 10 min in 100% solvent B and for 10 min in 100% solvent A. The ESI emitter, a gold-coated fused silica (5 cm × 25 μm ID × 360 μm OD, Nanoseparations), was heated to 195 °C. A high voltage of 2 kV was applied for stable spray operation. The LC pump, the mass spectrometer as well as the automatic mass spectra acquisitions were controlled using the Xcaliburtm 1.2 system software (Thermo). The MS/MS ions search was carried out in UniProtKB databases using MASCOT. Taxonomy was limited to Homo sapiens, peptide precursor charge was set to 2+ or 3+, mass tolerance of ±1.2 Da for precursor peptide and ±0.6 Da for fragment peptides was allowed and the number of accepted missed cleavage sites was set to one. Alkylation of cysteine by carbamidomethylation was taken as a fixed modification, while oxidation and phosphorylation were considered as possible modifications. We consider significant peptides with individual ion scores ($-10 \times \log[P]$, where P is the probability that the observed match is a random event) that indicate identity ($p < 0.05$).

Western blotting analysis of proteomic candidates

Cell conditions were the same as those of the DIGE experiments. Samples (30 μg) were separated by 12% SDS-PAGE and transferred onto a PVDF membrane (Millipore). To confirm the results obtained from 2D-DIGE analysis, the relative amount of NAP1L1 and Ubiquilin-1 proteins were assessed by Western blot with appropriate monoclonal antibodies (TemaRicerca). For quantification we used blots that were stained with Coomassie brilliant blue R-250 and subjected to densitometric analysis using Quantity One Software (Bio-Rad). Statistical analysis of the data was performed by Student's t-test; p-values 0.05 were considered statistically significant. The intensities of the immunostained bands were normalized with the total protein intensities measured by Coomassie brilliant blue R-250 from the same blot.

Conclusions

Our study is one of the few works that have investigated in detail the interaction of two pro-drugs using a wide, quantitative proteomic approach. Proteomics methods have the potential to provide specific insight into the alterations induced by drugs on protein expression. In turn, the observed proteomic alterations may be related to the modes of action of the drugs themselves. We have used such an approach to investigate the molecular mechanisms through which two cytotoxic gold based drugs

i.e. AuL12 and Au_2Phen cause their biological effects. Our proteomic results suggest the putative targets of these compounds. In particular we found that both treatments cause an over-expression of Ubiquilin-1 involved in inhibiting protein degradation. The cytotoxic effects of the two gold-compounds could be related to an impairment of protein degradation pathway. Comparing these results with the previously reported[15] we notice that the functions of some proteins could be correlated. The first correlation is between two proteins that are involved in RNA processing. In A2780/S cells treated with AuL12 we observed a down-regulation of the STRAP (Spot 6) which plays a role in the cellular distribution of the complex required for pre-mRNA splicing. Otherwise in the same cells treated with Auoxo 6 and Auranofin[15] we found down regulated the heterogeneous nuclear ribonucleoprotein H, a component of the heterogeneous nuclear ribonucleoprotein (hnRNP) complexes which mediates pre-mRNA alternative splicing regulation. The second correlation we found is between two proteins involved in connections of cytoskeletal components to membrane. In this paper we identified as overexpressed the protein Ubiquilin-1 (Spot 15) that links CD47 to the cytoskeleton and promotes the surface expression of GABA-A receptors. In the previous work, we found an over-expression of the protein Ezrin, required in epithelial cells for the formation of microvilli and therefore involved in connections of major cytoskeletal structures to the plasma membrane. Further differential proteomics analysis likely using different cancer cell lines will be necessary to identify common trends among gold(III) complexes and with respect to gold(I). Extending the analysis to the transcription level will better explain whether the observed differences in protein amounts are caused by transcriptional or post-translational events. Overall, these findings may contribute to elucidate the molecular mechanisms of the tested drugs and offer insight into their respective modes and sites of biological action.

Notes

FG and MP performed the 2-DIGE gels and mass spectrometry and analyzed the data, CG analyzed the data, IL performed cell cultures, TG analyzed the 2-DIGE data, DF provided the AuL12, MAC provided the Au2Phen, EM contributed cell reagents, LB contributed reagents, materials analysis tools and in writing the paper, PAM analyzed the data and contributed in writing the paper, AM and LM analyzed the data and wrote the paper.

FG received a fellowship from Consorzio Interuniversitario di Ricerca in Chimica dei Metalli nei Sistemi Biologici (C.I.R.C.M.S.B). This work was supported by grants to LM from Beneficentia Stiftung and Regione Toscana (NANO-TREAT project) and by grants to LB and AM from the FIRB project "Italian Human ProteomeNet" (BRN07BMCT_013), from Italian Ministry of University and Scientific Research.

References

1 A. Jemal, R. Siegel, J. Xu and E. Ward, *Ca-Cancer J. Clin.*, 2010, **60**(5), 277–300.
2 B. A. Goff, L. S. Mandel, C. W. Drescher, N. Urban, S. Gough, K. M. Schurman, J. Patras, B. S. Mahony and M. R. Andersen, *Cancer*, 2007, **109**(2), 221–227.
3 K. M. Hajra, L. Tan and J. R. Liu, *Adv. Exp. Med. Biol.*, 2008, **622**, 197–208.
4 R. Agarwal and S. B. Kaye, *Nat. Rev. Cancer*, 2005, **8**, 311–321.
5 P. C. Bruijnincx and P. J. Sadler, *Curr. Opin. Chem. Biol.*, 2008, **12**, 197.
6 S. Nobili, E. Mini, I. Landini, C. Gabbiani, A. Casini and L. Messori, *Med. Res. Rev.*, 2010, **30**(3), 550–580.
7 A. Casini, C. Hartinger, C. Gabbiani, E. Mini, P. J. Dyson, B. K. Keppler and L. Messori, *J. Inorg. Biochem.*, 2008, **102**, 564.
8 A. Casini, M. A. Cinellu, G. Minghetti, C. Gabbiani, M. Coronnello, E. Mini and L. Messori, *J. Med. Chem.*, 2006, **49**, 5524–5531.
9 C. Gabbiani, A. Casini, L. Messori, A. Guerri, M. A. Cinellu, G. Minghetti, M. Corsini, C. Rosani, P. Zanello and M. Arca, *Inorg. Chem.*, 2008, **47**, 2368–2379.
10 C. Marzano, L. Ronconi, F. Chiara, M. C. Giron, I. Faustinelli, P. Cristofori, A. Trevisan and D. Fregona, *Int. J. Cancer*, 2011, **129**(2), 487–496.
11 M. A. Cinellu, L. Maiore, M. Manassero, A. Casini, M. Arca, H. H. Fiebig, G. Kelter, E. Michelucci, G. Pieraccini, C. Gabbiani and L. Messori, *ACS Med. Chem. Lett.*, 2010, **1**(7), 336–339.
12 Y. Wang and J. F. Chiu, *Met.-Based Drugs*, 2008, **2008**, 716329.
13 N. B. Larbi and C. Jefferies, *Methods Mol. Biol.*, 2009, **517**, 105–132.
14 W. Weiss and A. Gorg, *Methods Mol. Biol.*, 2009, **564**, 13–32.
15 F. Magherini, A. Modesti, L. Bini, M. Puglia, I. Landini, S. Nobili, E. Mini, M. A. Cinellu, C. Gabbiani and L. Messori, *J. Biol. Inorg. Chem.*, 2010, **15**(4), 573–582.
16 P. Skehan, *J. Natl. Cancer Inst.*, 1990, **82**, 1107–1112.
17 N. R. Hope and G. I. Murray, *Hum. Pathol.*, 2011, **42**(3), 393–402.
18 T. Fukuda, H. Oyamada, T. Isshiki, M. Maeda, T. Kusakabe, A. Hozumi, T. Yamaguchi, T. Igarashi, H. Hasegawa, T. Seidoh and T. Suzuki, *J. Histochem. Cytochem.*, 2007, **55**(4), 335–345.
19 B. F. Krasnikov, C. H. Chien, R. Nostramo, J. T. Pinto, E. Nieves, M. Callaway, J. Sun, K. Huebner and A. J. Cooper, *Biochimie*, 2009, **91**(9), 1072–1080.
20 Y. Kuramitsu, B. Baron, S. Yoshino, X. Zhang, T. Tanaka, M. Yashiro, K. Hirakawa, M. Oka and K. Nakamura, *Anticancer Res.*, 2010, **30**(11), 4459–4465.
21 M. Kidd, I. M. Modlin, S. M. Mane, R. L. Camp, G. Eick and I. Latich, *Ann. Surg. Oncol.*, 2006, **3**(2), 253–262.
22 S. W. Kim, S. Kim, E. J. Nam, Y. W. Jeong, S. H. Lee, J. H. Paek, J. H. Kim, J. W. Kim and Y. T. Kim, *OMICS*, 2011, **5**(5), 281–292.
23 J. E. Reiner and P. K. Datta, *Front. Biosci.*, 2011, **16**, 105–115.
24 J. T. Fox, K. Y. Lee and K. Myung, *FEBS Lett.*, 2011, **585**(18), 2780–2785.
25 S. Romain, P. O. Bendahl, O. Guirou, P. Malmström, P. M. Martin and M. Fernö, *Int. J. Cancer*, 2001, **95**(1), 56–61.
26 F. Magherini, A. Modesti, L. Bini, M. Puglia, I. Landini, S. Nobili, E. Mini, M. A. Cinellu, C. Gabbiani and L. Messori, *J. Biol. Inorg. Chem.*, 2010, **15**(4), 573–582.
27 Y. Liu, R. F. Tian, Y. M. Li, W. P. Liu, L. Cao, X. L. Yang, W. D. Cao and X. Zhang, *Brain Res.*, 2010, **1336**, 98–102.
28 J. Lee, *Arch. Pharmacal Res.*, 2010, **33**(9), 1401–1409.
29 M. Krockenberger, J. B. Engel, J. Kolb, Y. Dombrowsky, S. F. Häusler, N. Kohrenhagen, J. Dietl, J. Wischhusen and A. Honig, *J. Cancer Res. Clin. Oncol.*, 2010, **136**(5), 651–657.
30 K. Patel, E. C. Farlow, A. W. Kim, B. S. Lee, S. Basu, J. S. Coon, D. DeCresce, L. Thimothy, K. A. Walters, C. Fhied, C. Chang, S. H. Chen, L. P. Faber, P. Bonomi, M. J. Liptay and J. A. Borgia, *Int. J. Cancer*, 2011, **129**(1), 133–142.
31 H. E. Moore, E. L. Davenport, E. M. Smith, S. Muralikrishnan, A. S. Dunlop, B. A. Walker, D. Krige, A. H. Drummond, L. Hooftman, G. J. Morgan and F. E. Davies, *Mol. Cancer Ther.*, 2009, **8**(4), 762–770.
32 L. Ronconi, L. Giovagnini, C. Marzano, F. Bettio, R. Graziani, G. Pilloni and D. Fregona, *Inorg. Chem.*, 2005, **44**(6), 1867–1881.
33 M. M. Bradford, *Anal. Biochem.*, 1976, **72**, 248–254.
34 D. F. Hochstrasser, A. Patchornik and C. R. Merril, *Anal. Biochem.*, 1988, **173**, 412–423.
35 U. Hellman, C. Wernstedt, J. Gonez and C. H. Heldin, *Anal. Biochem.*, 1995, **224**, 451–455.
36 V. Soskic, M. Gorlach, S. Poznanovic, F. D. Boehmer and J. Godovac-Zimmermann, *Biochemistry*, 1999, **38**, 1757–1764.
37 H. D. Meiring, E. van der Heeft, G. J. ten Hove and A. P. J. M. de Jong, *J. Sep. Sci.*, 2002, **25**, 557–568.